



The East Greenland Spill Jet as an important component of the Atlantic Meridional Overturning Circulation

Wilken-Jon von Appen^{a,*}, Inga M. Koszalka^b, Robert S. Pickart^c, Thomas W.N. Haine^b, Dana Mastropole^d, Marcello G. Magaldi^{b,e}, Héðinn Valdimarsson^f, James Girton^g, Kerstin Jochumsen^h, Gerd Krahmannⁱ

^a Alfred Wegener Institute, Helmholtz Centre for Polar and Marine Research, Am Handelshafen 12, 27570 Bremerhaven, Germany

^b Department of Earth and Planetary Sciences, Johns Hopkins University, Baltimore, MD, USA

^c Department of Physical Oceanography, Woods Hole Oceanographic Institution, Woods Hole, MA, USA

^d MIT-WHOI Joint Program in Oceanography, Cambridge/Woods Hole, MA, USA

^e Institute of Marine Sciences, National Research Council, Lerici, La Spezia, Italy

^f Marine Research Institute, Reykjavik, Iceland

^g Applied Physics Laboratory, University of Washington, Seattle, WA, USA

^h Institute of Oceanography, University of Hamburg, Hamburg, Germany

ⁱ GEOMAR, Helmholtz Centre for Ocean Research, Kiel, Germany

ARTICLE INFO

Article history:

Received 4 April 2014

Received in revised form

3 June 2014

Accepted 10 June 2014

Available online 19 June 2014

Keywords:

East Greenland Spill Jet

Denmark Strait overflow water

Atlantic Meridional Overturning Circulation

Shelf Basin interaction

ABSTRACT

The recently discovered East Greenland Spill Jet is a bottom-intensified current on the upper continental slope south of Denmark Strait, transporting intermediate density water equatorward. Until now the Spill Jet has only been observed with limited summertime measurements from ships. Here we present the first year-round mooring observations demonstrating that the current is a ubiquitous feature with a volume transport similar to the well-known plume of Denmark Strait overflow water farther downslope. Using reverse particle tracking in a high-resolution numerical model, we investigate the upstream sources feeding the Spill Jet. Three main pathways are identified: particles flowing directly into the Spill Jet from the Denmark Strait sill; particles progressing southward on the East Greenland shelf that subsequently spill over the shelfbreak into the current; and ambient water from the Irminger Sea that gets entrained into the flow. The two Spill Jet pathways emanating from Denmark Strait are newly resolved, and long-term hydrographic data from the strait verifies that dense water is present far onto the Greenland shelf. Additional measurements near the southern tip of Greenland suggest that the Spill Jet ultimately merges with the deep portion of the shelfbreak current, originally thought to be a lateral circulation associated with the sub-polar gyre. Our study thus reveals a previously unrecognized significant component of the Atlantic Meridional Overturning Circulation that needs to be considered to understand fully the ocean's role in climate.

© 2014 Elsevier Ltd. All rights reserved.

1. Introduction

Strong air–sea heat exchange in the Nordic Seas leads to the formation of dense water which is exported to the Atlantic Ocean through the Faroe Bank Channel and the Denmark Strait. These overflows form the headwaters of the Deep Western Boundary Current (DWBC) (Dickson and Brown, 1994), which constitutes the abyssal limb of the Atlantic Meridional Overturning Circulation (AMOC). The largest and densest overflow plume emanates from Denmark Strait and entrains ambient water from the Irminger Sea.

During this process energetic cyclones are formed that rapidly propagate with the overflow water southward along the East Greenland continental slope (Spall and Price, 1998; Käse et al., 2003; von Appen et al., 2014). Recently, a narrow current transporting intermediate density water equatorward was discovered inshore of the Denmark Strait overflow plume. This feature was termed the East Greenland Spill Jet (hereafter referred to simply as the Spill Jet), owing to the hypothesis that its formation is associated with dense water spilling off the shelf and forming a gravity current south of Denmark Strait (Pickart et al., 2005). Model simulations and subsequent observations support this hypothesis (Magaldi et al., 2011; Harden et al., 2014).

To date the Spill Jet has only been observed from a small number of quasi-synoptic shipboard velocity sections, all of them

* Corresponding author. Tel.: +49 471 4831 2903.

E-mail address: Wilken-Jon.von.Appen@awi.de (W.-J. von Appen).

occupied during the summer months near 65°N (labeled the “Spill Jet section”, Fig. 1). From these limited data it has been suggested that the Spill Jet is located on the upper slope and transports between 3 and 7 Sv ($1 \text{ Sv} = 10^6 \text{ m}^3/\text{s}$) equatorward (Brearley et al., 2012). For the most part, its density is lighter than 27.8 kg/m^3 (all densities in this paper are potential densities referenced to the surface), which is commonly taken as the upper limit of Denmark Strait overflow water (DSOW). However, hydrographic measurements (Rudels et al., 1999; Macrandar et al., 2005; Brearley et al., 2012; Falina et al., 2012) and numerical simulations (Koszalka et al., 2013) suggest that dense water cascading off the shelf south of Denmark Strait can at times contribute to the deeper DSOW plume. Basic questions thus remain about the existence and importance of the Spill Jet and its relation to the circulation of the North Atlantic Ocean (Fig. 1). After describing the data and methods employed in the study, we demonstrate the ubiquity of the Spill Jet, investigate its formation region and mechanisms, and close with an assessment of its contribution to the AMOC.

2. Data and methods

2.1. Mooring array

Seven moorings were deployed along the Spill Jet section (named consecutively from “EG1” on the shelf in 248 m at 65°30.0'N 33°8.8'W to “EG7” on the slope in 1585 m at 65°7.3'N 32°41.1'W, Fig. 1) from 4 September 2007 to 4 October 2008 (von Appen et al., 2014). The moorings contained conductivity–temperature–depth (CTD) moored profilers operating between the bottom and $\approx 100 \text{ m}$ depth. On the outer three moorings (EG5–7) the profilers included an acoustic current meter. Acoustic Doppler current profilers (ADCPs) measured velocity on all moorings

between $\approx 100 \text{ m}$ and the surface, and also between $\approx 100 \text{ m}$ and the bottom on the inner four moorings (EG1–4). Some of the moored profilers stopped working prematurely, but the mean section is robust (see von Appen, 2012).

The dominant signal in the mooring records was the passage of Denmark Strait Overflow Water (DSOW) cyclones every few days. These features contain lenses of dense overflow water on the bottom with a strong azimuthal flow in the water column above (von Appen et al., 2014). We identified the DSOW cyclone passages based on a set of criteria involving their velocity signal (translational and azimuthal), their density signature (the presence of anomalously dense water), and mooring motion (the strong flow near the centers of the cyclones resulted in mooring blow-down). It was found that the influence of the cyclones extended less than 18 h before and after their centers passed by the array. In order to isolate the Spill Jet signature, we identified the time periods when cyclones were present and excluded them from consideration. The mean potential density section in the absence of cyclones ($\approx 35\%$ of the record) was computed using a Laplacian spline interpolator with tension (Pickart and Smethie, 1998). Thermal wind was used to provide the geostrophic shear which was referenced to the mean cyclone-free along-slope velocities at the moorings (in the middle of the water column, the velocity records are complete enough to calculate the means). This absolute geostrophic velocity was then gridded with the same spline interpolator. The standard error of the Spill Jet transport is estimated using an integral time scale of several hours (von Appen et al., 2014). At least 25 independent realizations went into the Spill Jet quantification and most locations are defined by many more realizations. Dividing the standard deviation by the square root of the minimum number of degrees of freedom gives a standard error of $< 0.7 \text{ Sv}$. Instrument errors, assumed to be uncorrelated across the array, add $< 0.1 \text{ Sv}$ uncertainty (Nikolopoulos et al., 2009).

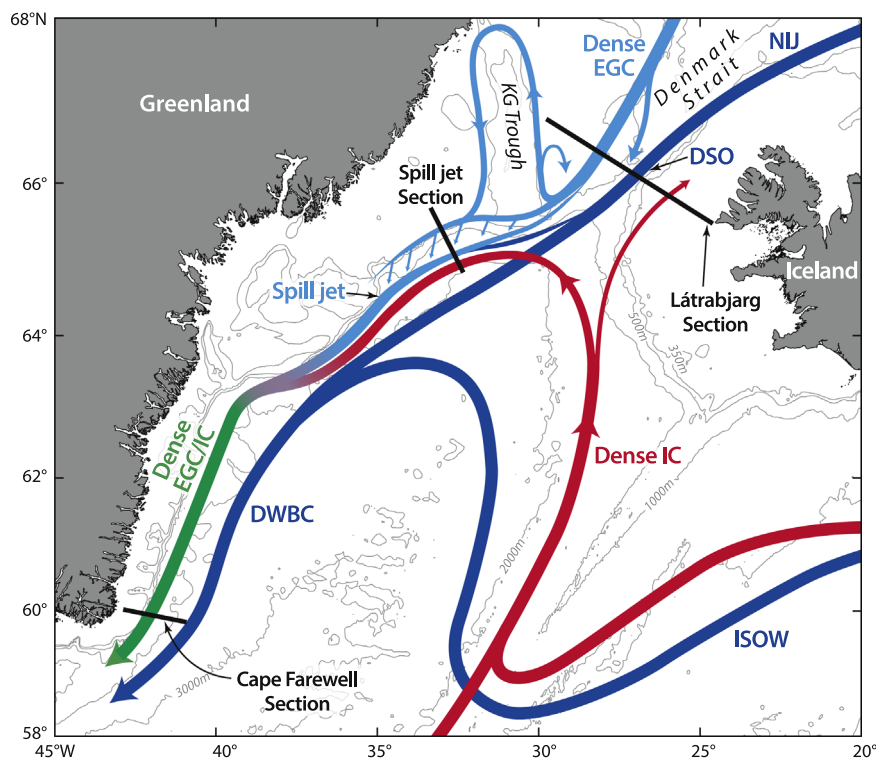


Fig. 1. Schematic of the dense water pathways in the Irminger Sea. This roughly corresponds to waters with density $> 27.6 \text{ kg/m}^3$. The abbreviations are as follows: EGC, East Greenland Current; NIJ, North Icelandic Jet; DSO, Denmark Strait Overflow; IC, Irminger Current; ISOW, Iceland Scotland Overflow Water; DWBC, Deep Western Boundary Current; and KG Trough, Kangerdlugssuaq Trough. Note that the less dense surface circulation of the IC, the EGC, and the East Greenland Coastal Current is not shown.

Table 1

List of hydrographic transects along the Látrabjarg section. The abbreviations of the ship names and their countries are given in (a) and the individual cruises contributing to the mean Látrabjarg section are given in (b).

(a) Abbrev.	Ship name	Country
A	Árni Friðriksson	Iceland
AR	Aranda	Finland
B	Bjarni Sæmundsson	Iceland
D	Discovery	United Kingdom
JR	James Clark Ross	United Kingdom
KN	Knorr	United States
M	Meteor	Germany
MSM	Maria S. Merian	Germany
P	Poseidon	Germany
PS	Polarstern	Germany

(b)					
Date	Cruise	Date	Cruise	Date	Cruise
March 1990	B-03-1990	May 1998	B-06-1998	November 2005	B-13-2005
August 1990	B-13-1990	August 1998	A-09-1998	February 2006	B-02-2006
November 1990	B-17-1990	September 1998	B-09-1998	May 2006	B-04-2006
February 1991	B-03-1991	September 1998	P-244	September 2006	D-311
May 1991	B-07-1991	September 1998	P-244	November 2006	A-11-2006
September 1991	A-12-1991	September 1998	P-244	February 2007	B-03-2007
November 1991	B-14-1991	October 1998	PS-52	May 2007	B-08-2007
February 1992	B-02-1992	November 1998	B-12-1998	July 2007	MSM-05-4
May 1992	B-07-1992	February 1999	B-02-1999	August 2007	B-11-2007
September 1992	A-08-1992	May 1999	B-07-1999	November 2007	A-14-2007
September 1992	B-14-1992	August 1999	A-10-1999	February 2008	A-01-2008
October 1992	B-16-1992	September 1999	B-13-1999	May 2008	B-08-2008
February 1993	B-02-1993	November 1999	B-16-1999	August 2008	A-11-2008
May 1993	B-07-1993	February 2000	B-02-2000	October 2008	KN-194
August 1993	A-14-1993	May 2000	B-06-2000	November 2008	A-13-2008
September 1993	B-11-1993	August 2000	B-10-2000	February 2009	B-01-2009
October 1993	B-14-1993	November 2000	B-14-2000	May 2009	B-05-2009
February 1994	B-03-1994	February 2001	B-02-2001	June 2009	MSM-12-1
May 1994	B-08-1994	May 2001	B-06-2001	August 2009	B-10-2009
September 1994	B-14-1994	August 2001	B-10-2001	November 2009	A-14-2009
October 1994	B-17-1994	November 2001	B-14-2001	February 2010	B-04-2010
March 1995	B-03-1995	May 2002	B-05-2002	May 2010	B-08-2010
May 1995	B-07-1995	August 2002	B-09-2002	July 2010	M-82-1
August 1995	A-11-1995	September 2002	P-294	August 2010	B-12-2010
September 1995	B-14-1995	November 2002	A-10-2002	February 2011	B-01-2011
November 1995	B-17-1995	February 2003	A-02-2003	May 2011	B-04-2011
February 1996	B-03-1996	May 2003	A-09-2003	August 2011	M-85-2
August 1996	A-11-1996	August 2003	B-03-2003	August 2011	KN-203
October 1996	A-14-1996	September 2003	P-303	December 2011	B-10-2011
February 1997	B-03-1997	November 2003	B-10-2003	February 2012	B-02-2012
May 1997	B-06-1997	February 2004	B-01-2004	May 2012	B-05-2012
August 1997	A-14-1997	May 2004	B-05-2004	June 2012	MSM-21-1b
August 1997	AR-34	November 2004	B-15-2004	July 2012	JR-267
September 1997	AR-34	February 2005	B-02-2005	August 2012	P-437
September 1997	B-10-1997	May 2005	B-06-2005	August 2012	B-09-2012
November 1997	B-15-1997	August 2005	A-09-2005		
February 1998	B-02-1998	August 2005	P-327		

2.2. Hydrographic sections

We use a collection of 109 CTD sections occupied between 1990 and 2012 along the “Látrabjarg section” (66°46.0′N 29°45.8′W to 65°29.1′N 25°35.9′W) across Denmark Strait (Fig. 1). A detailed list of the individual occupations at the Látrabjarg section is given in Table 1. Not all occupations cover the entire section, but a sensitivity test indicated that this does not qualitatively change the mean. Each section was interpolated onto a standard grid with the same horizontal and vertical resolution (2.5 km and 10 m, respectively) using a Laplacian spline interpolator with tension (Pickart and Smethie, 1998). We also use a collection of 36 CTD sections in the vicinity of the WOCE A1E/AR7E line (marked as “Cape Farewell section” in Fig. 1) occupied between 1991 and 2007. These sections are detailed in Table 1 of Våge et al. (2011). The absolute geostrophic velocity at the Cape Farewell section was referenced using AVISO absolute sea surface height data, the

accuracy of which was assessed using available shipboard ADCP data (see Våge et al., 2011).

2.3. Numerical circulation model

A hydrostatic version of the Massachusetts Institute of Technology general circulation model (MITgcm) is used. The configuration has a horizontal grid spacing of 2 km and 210 levels in the vertical (grid cell height ranging from 2 m at the surface to 15 m at depths greater than 100 m). There are three open boundaries (69.8°N, 10.2°W, and 60.3°N); the western boundary is closed at the east coast of Greenland. The boundary conditions for hydrography and velocity are obtained from the 1/12° resolution North-Atlantic non-tidal experiment of the Hybrid Coordinate Ocean Model (HYCOM) (Chassignet et al., 2009). No-slip conditions are applied to all material boundaries. The NCEP reanalysis (Kalnay et al., 1996) provides the atmospheric forcing. The simulation

spans the summer of 2003 (from 1 July to 15 October). The model uses partial bottom cells and a rescaled height coordinate (Adcroft and Campin, 2004) to accurately simulate the boundary current on the continental slope in the Irminger Basin. It also features a nonlinear free surface, a flow-dependent Leith biharmonic viscosity, a third-order advection scheme with zero explicit diffusivity for tracers, and vertical mixing using the *K*-profile parameterization (Large et al., 1994).

2.4. Lagrangian particle model

Lagrangian particles are deployed in the numerical circulation model at the Spill Jet section and their trajectories are simulated offline using the three-dimensional velocity fields from the model (see Koszalka et al., 2013 for a detailed validation of this method). The code uses a trapezoidal solver with a 2nd-order predictor and a 3rd-order corrector scheme. At boundaries, the normal velocity component of the particle vanishes and the particle slides freely. At each time step, the velocity is linearly interpolated to the particle positions. The time series of temperature and salinity along the trajectories are obtained by linear interpolation at each time step. Previous use of this trajectory scheme has resulted in favorable comparisons to observations (Koszalka et al., 2013).

3. The ubiquitous East Greenland Spill Jet

In the absence of the DSOW cyclones, the Spill Jet is clearly revealed in the composite mean absolute geostrophic velocity section (Fig. 2a; the absolute geostrophic velocity is qualitatively the same as the direct velocity measurements where they exist). This is the first robust, long-term evidence of the Spill Jet and firmly establishes it as a ubiquitous feature of the circulation south of Denmark Strait. The mooring observations were also averaged over shorter time periods and no discernible seasonal differences were found, which is similar to the lack of seasonality in DSOW cyclone properties observed at the same location (von Appen et al., 2014). The isopycnals in the year-long mean section are banked strongly upwards toward the slope and the associated thermal wind shear results in a strong, bottom-intensified flow reaching 0.45 m/s at 700 m depth. For the present study we define the Spill Jet as the deep flow within 28 km of the shelfbreak (offshore of this distance, the velocities are very small) in the density range 27.6–27.8 kg/m³ (Fig. 2a). The choice of the upper isopycnal distinguishes the Spill Jet from the warm and salty shallow flow of the East Greenland/Irminger Current (EGC/IC), while the lower isopycnal separates the Spill Jet from the DWBC that transports DSOW. We note that this density range is within the southward flowing component of the AMOC (Holliday et al., 2009; Lherminier et al., 2010; Sarafanov et al., 2012).

As noted earlier, there is evidence that dense water from the shelf can sometimes feed the upper part of the DWBC, and our mean section is consistent with this as well (the offshore, deepest part of the velocity signal is denser than 27.8, Fig. 2a). Hence it is difficult to define the boundary between the Spill Jet and the DWBC unambiguously. However, the bulk of the DSOW at the Spill Jet section is located seaward of the 1200 m isobath and coincides with a clear (distinct) velocity signal of the DWBC (Dickson and Brown, 1994; Brearley et al., 2012; Koszalka et al., 2013). Thus, using the 27.8 isopycnal for the lower limit of the Spill Jet allows us to distinguish it from the deep plume of overflow water emanating from Denmark Strait. With these bounds, we estimate the mean transport of the Spill Jet as the sum of the calculated along-slope absolute geostrophic velocities as shown in Fig. 2a. It is 3.3 ± 0.7 Sv of intermediate-density water flowing equatorward. This value is in the lower range of previous synoptic estimates

(Brearley et al., 2012), but it is two-thirds as large as the transport (≈ 5 Sv) of the DWBC at this latitude (Dickson and Brown, 1994). We note that even when DSOW cyclones are present, an average background flow exists that is consistent in magnitude and structure with the Spill Jet in Fig. 2a (von Appen et al., 2014; Magaldi et al., 2011). As such, we assume that the above transport estimate applies to the year-long record.

The regional numerical model employed here has been used previously to study the East Greenland boundary current system in summer 2003 (Magaldi et al., 2011; Koszalka et al., 2013). The earlier studies demonstrated that the model's deep circulation both from a Eulerian and a Lagrangian perspective is realistic, and its hydrographic properties agree with shipboard observations from summer 2003. In the present study this same simulation is used to investigate aspects of the Spill Jet that cannot be addressed with the mooring data. Note that we are not attempting to simulate the precise conditions measured by the array deployed from 2007 to 2008. Rather, we aim to shed light on the physical processes and basic circulation. The model-data comparisons below thus focus on the general characteristics and statistics of the flow, seeking qualitative agreement.

Consistent with our mooring records, the flow along the continental slope in the model south of the strait is dominated by the passage of DSOW cyclones (Magaldi et al., 2011). To isolate the signal of the Spill Jet in the model, we therefore implemented the same procedure for identifying cyclones and constructed the corresponding composite mean section of absolute geostrophic velocity in the absence of these features (Fig. 2b). The Spill Jet is clearly captured by the model. In light of the fact that the observations span a full year and the model covers only three months (during a different year), the qualitative agreement between the two mean sections is impressive. In both cases the Spill Jet is bottom intensified, with its core on the upper continental slope, and the isopycnals are banked strongly upwards toward the shelfbreak. As in the observations, the velocity core in the model is composed of water that is lighter than DSOW. The flow in the model is, however, generally faster than the mooring observations. Choosing the same isopycnal range of 27.6–27.8 for the model Spill Jet results in a transport roughly a factor of two larger than the observations. Possible reasons for this difference, such as interannual variability in the Denmark Strait overflow, variability in the wind stress associated with different phases of the North Atlantic Oscillation, and the influence of the model boundary conditions, were investigated. However, none of these can explain the difference in the Spill Jet transport between the data and the model.

4. Formation of the Spill Jet

The traditional view of the DSOW is that it flows through the deepest part of the Denmark Strait sill and forms a plume that descends the continental slope and feeds the DWBC (Smith, 1975; Price and O'Neil Baringer, 1994). Our long-term measurements of the Spill Jet advecting intermediate density water to the south—inshore of the overflow plume—thus beg the question: What is the origin of this water (which at times can be denser than 27.8)? The flow through Denmark Strait is known to be highly turbulent and energetic on timescales of a few days (Macrandar et al., 2005; Haine, 2010; Jochumsen et al., 2012). This makes it difficult to characterize the flow and the water masses in the strait using synoptic shipboard sections, and no mooring arrays have been deployed across the entire strait. In order to smooth out the mesoscale variability, we gathered all known shipboard hydrographic sections near the sill and constructed a mean transect across the strait. The mean section along the Látrabjarg section

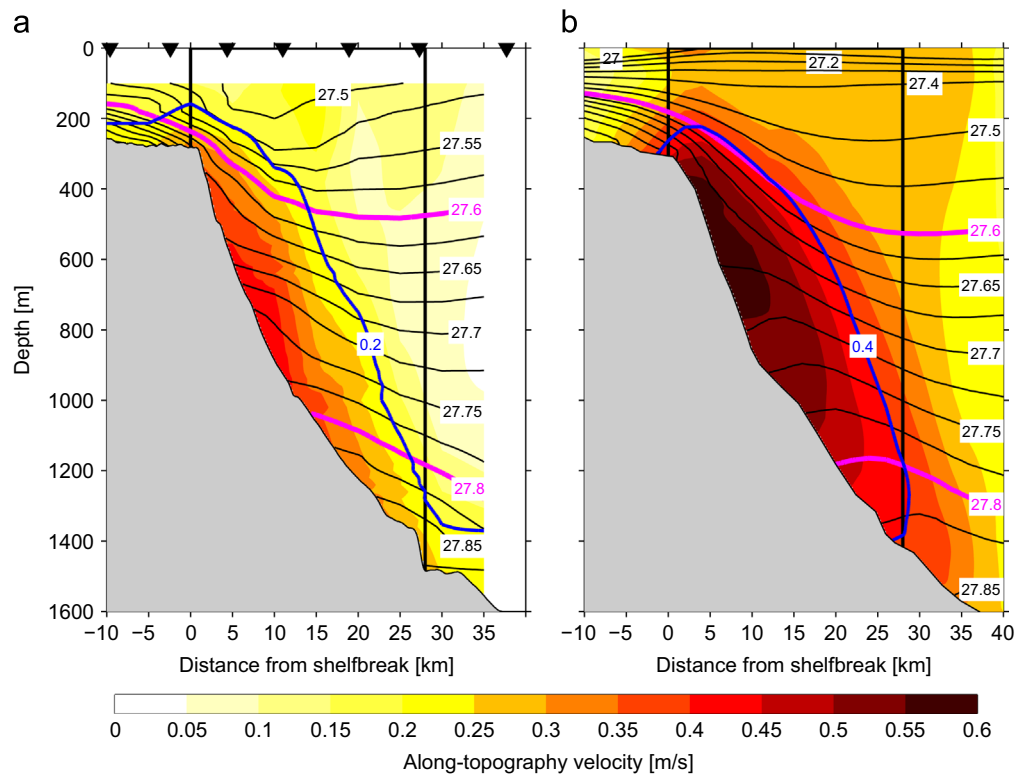


Fig. 2. Mean hydrography and velocity at the Spill Jet section. The means are constructed at the times when DSOW cyclones are absent. The equatorward absolute geostrophic velocity is shown in color and the blue contour and is overlain by potential density (kg/m^3) in black contours. (a) is from the mooring observations and (b) is from the numerical model. The Spill Jet is defined as the flow within 28 km of the shelfbreak (vertical black lines) in the density range 27.6–27.8 (magenta isopycnals). The absolute geostrophic velocity is referenced to the measured velocities and model velocities, respectively (an example of modeled along topography velocity is shown in Fig. 4b). The locations of the moorings are marked by inverted black triangles. (For interpretation of the references to color in this figure caption, the reader is referred to the web version of this paper.)

(Fig. 3) consists of 109 crossings occupied in all seasons spanning the time period 1990–2012.

The presence of the dense DSOW is clearly seen in the mean section, banked against the western side of the deepest part of the Denmark Strait sill (Fig. 3). The strong isopycnal tilt implies increased southward speed of the overflow water with depth at this location. These aspects of the DSOW are not particularly surprising. However, while DSOW has previously been observed on the shelf in individual synoptic transects (Macrandner et al., 2005; Jochumsen et al., 2012), our mean hydrographic section (Fig. 3) robustly demonstrates the presence of dense water > 27.8 far onto the East Greenland shelf in a layer roughly 100 m thick (even the 27.9 isopycnal is found shoreward of the shelfbreak). Dense water on the shelf was seen in all sections that extended far onto the shelf (Fig. 3). Since the seasonal cycle of temperature and density in the dense water of Denmark Strait is small (0.09°C and 0.007 kg/m^3 , respectively; Jochumsen et al., 2012), possible seasonal biases in the CTD occupations on the East Greenland shelf do not change this picture significantly. This implies that some of the water in the DSOW density range exiting the Nordic Seas west of Iceland does not feed the traditional plume of overflow water stemming from the sill. In light of the evidence noted above regarding off-shelf transport of dense water south of Denmark Strait, one then wonders if the dense water on the shelf in the Látrabjarg section contributes to the Spill Jet.

To investigate this, particles were released at the Spill Jet section in the numerical model and tracked backwards in time. Previous studies (Magaldi et al., 2011; Koszalka et al., 2013), in conjunction with the favorable model/data comparison of the Spill Jet in Fig. 2, give us confidence that the model accurately represents the physical processes in the Irminger Sea and can be used to investigate the formation pathways of the Spill Jet. The

numerical particles were deployed within the current (Fig. 4) at times mid-way between the passage of consecutive DSOW cyclones. We use the seven independent deployment times between 10 September and the end of the simulation (15 October). In total, 1157 particles were released and tracked backwards in time until the particle either left the model domain or until the beginning of the model run (resulting in a tracking duration up to 71 days). The results do not change qualitatively after 20 days of tracking duration, demonstrating that the duration of our simulation is sufficient. Supplementary Movie 1 (available in the online version of this paper at <http://dx.doi.org/10.1016/j.dsr.2014.06.002>) shows a three dimensional view of the particles moving through the model domain, and Fig. 5 shows the locations of the particles 10 days prior to arriving at the Spill Jet section. In general, three main pathways contributing to the Spill Jet became apparent, which are highlighted in Fig. 6 as “pathway groups”. Blue particles cross the Látrabjarg section through the deepest part of the Denmark Strait sill (> 350 m bottom depth, indicated by the yellow line segment in Fig. 6) and never visit the East Greenland shelf. This is called the SILL-DIRECT group. Green particles spend time on the Greenland shelf and begin the simulation either upstream of the Látrabjarg section or downstream of it on the shelf. This is the EG SHELF group. Lastly, red particles start in the Irminger Basin and cross the zonal section as indicated in Fig. 6. This is the IRMINGER BASIN group. The trajectories of three typical particles from each of these groups are shown in Fig. 7.

The main conclusions from the reverse particle tracking are summarized in Fig. 8. About 11% of the particles (the SILL-DIRECT group) follow a direct pathway along the continental slope from the deepest part of Denmark Strait to the Spill Jet section (Fig. 8a), taking a median time of 8 days to travel the 280 km distance. These particles begin their trajectories in the Iceland Sea northeast

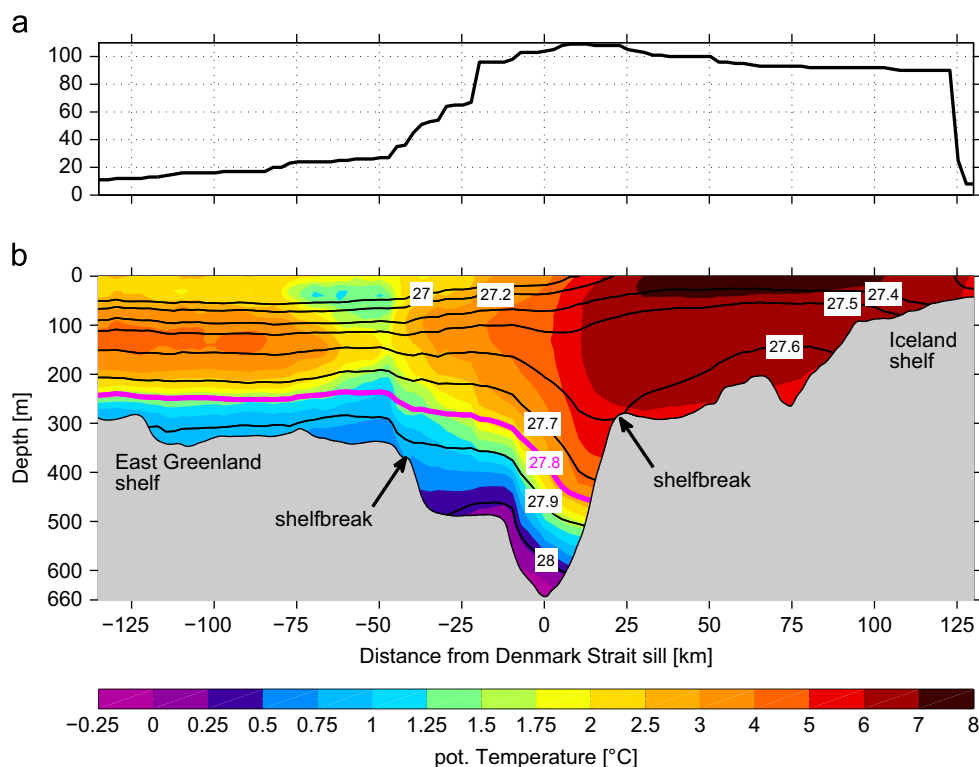


Fig. 3. Mean hydrography at the Látrabjarg section. The number of CTD occupations that the mean hydrography across Denmark Strait is based on is indicated in (a) and the mean is shown in (b). The potential temperature is shown in color and is overlain by potential density (kg/m^3) in contours. The 27.8 isopycnal, indicating the top of the DSOW layer, is highlighted in magenta. (For interpretation of the references to color in this figure caption, the reader is referred to the web version of this paper.)

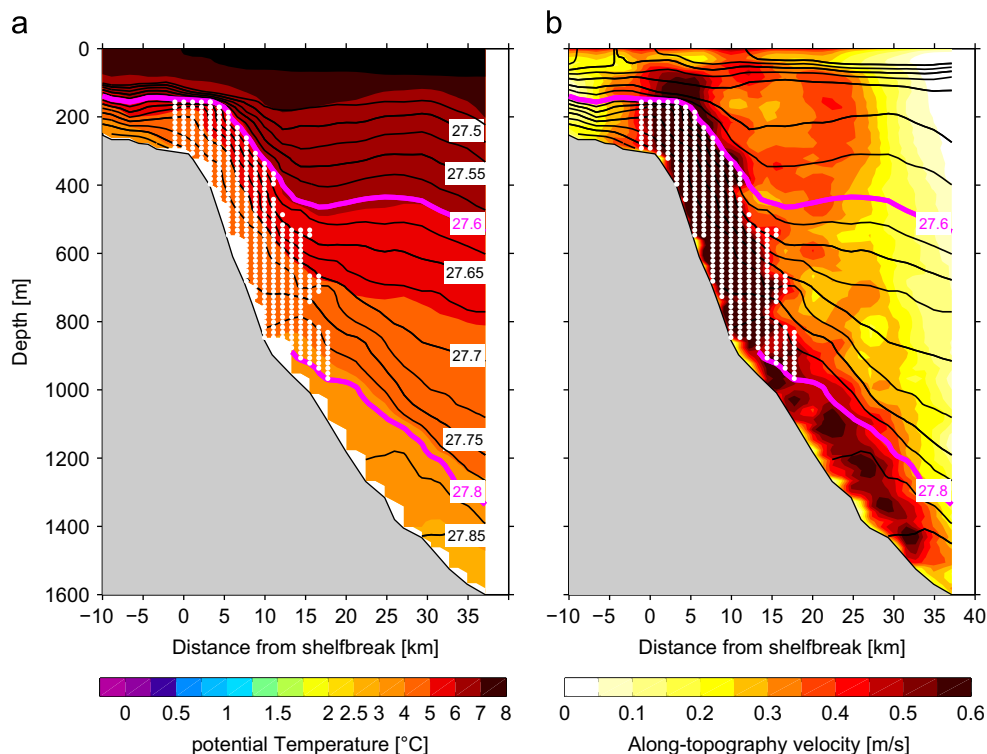


Fig. 4. Example of particle deployment locations. Representative example of a deployment of particles into the Spill Jet in the numerical model. Each of the white dots represents a particle released on 10 September 2003. The instantaneous (a) potential temperature and (b) along-topography velocity are shown in color overlain by potential density (kg/m^3) in contours. The density limits of the Spill Jet are denoted by the magenta contours. (For interpretation of the references to color in this figure caption, the reader is referred to the web version of this paper.)

of Denmark Strait, entering the strait along either the Iceland slope or the Greenland slope. Their density is reduced from > 28 in the vicinity of the strait to values around 27.7 near 65°N (Fig. 8b). This

pathway group indicates that the Spill Jet contains water that is in the traditional DSOW density range at the Denmark Strait sill. Hence, a portion of this water does not participate in the deep

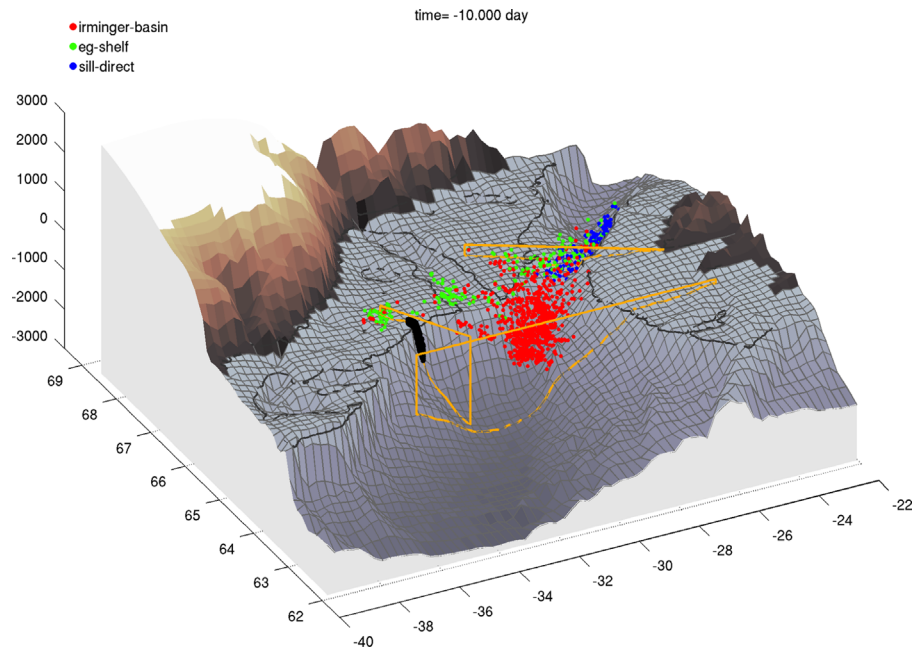


Fig. 5. 3D view of the model particles ten days prior to arriving at the Spill Jet section. The particles are colored according to the pathway groups. The Spill Jet section, the Látrabjarg section, and the Irminger Basin line are indicated in yellow. The locations of the particle deployments at the Spill Jet section are shown in black. The 350 m isobath and the coastline are drawn in black. The resolution of the bathymetry in the model is higher than shown in the figure. See also Movie 1 which spans the entire simulation. (For interpretation of the references to color in this figure caption, the reader is referred to the web version of this paper.)

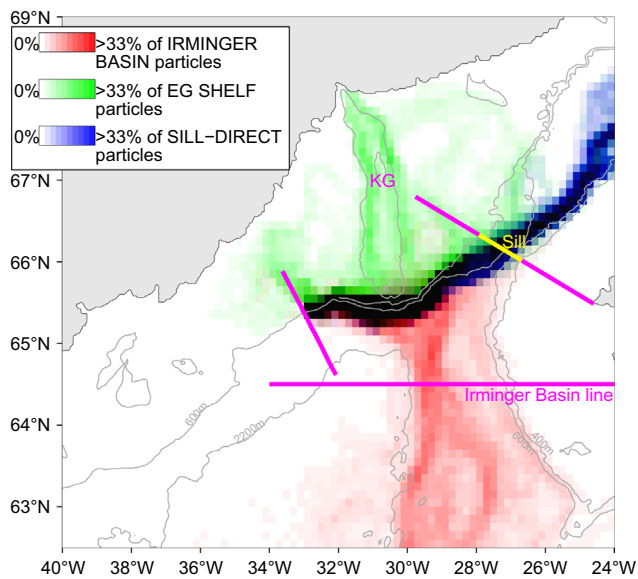


Fig. 6. Pathways of numerical particles feeding the Spill Jet. Pixels (0.1° of latitude by 0.2° of longitude) are colored by the percentage of particles of the pathway groups that visited the pixel during the simulation. The red channel of each pixel ranges from white when no IRMINGER BASIN particles visited the pixel to red when 33% or more of all IRMINGER BASIN particles visited the pixel. The green channel corresponds to the East Greenland SHELF pathways. The SILL-DIRECT pathway, from the Denmark Strait sill to the Spill Jet section, is shown by the blue channel. Black pixels were visited by many particles from all pathway groups. (For interpretation of the references to color in this figure caption, the reader is referred to the web version of this paper.)

plume that descends the continental slope immediately south of the strait, but instead feeds the Spill Jet higher on the slope.

Approximately 19% of the particles (the EG SHELF group) begin the simulation on the East Greenland shelf and/or north of the Látrabjarg section and at some point cascade off the shelf into the Spill Jet. The residence time on the shelf varies from days to weeks, and about 15% of these particles spend the entire simulation on

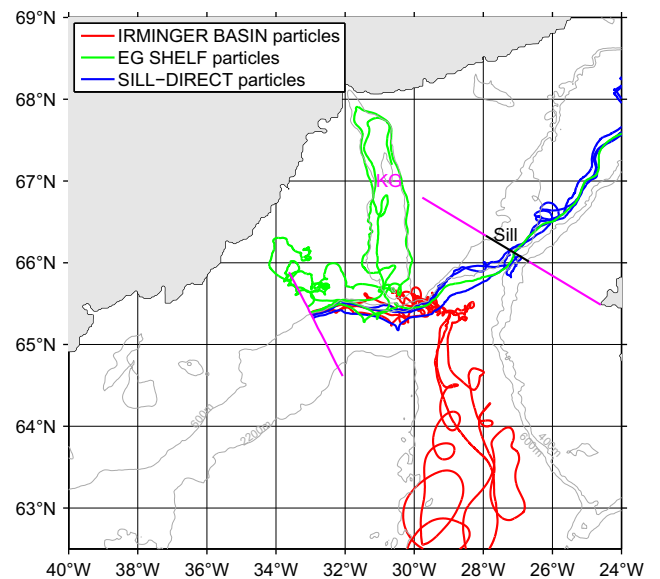


Fig. 7. Typical numerical particle trajectories. Three particles from each of the groups were subjectively selected to show typical trajectories of the different pathway groups.

the shelf prior to spilling near 65°N (Fig. 8a). A complex flow pattern on the shelf is evident in Fig. 6, with many particles circulating around the deep Kangerdlugssuaq Trough. The off-shelf spilling pathway revealed by these particles supports recent observational (Harden et al., 2014) and numerical (Magaldi et al., 2011; Koszalka et al., 2013) results, and is consistent with the presence of dense water on the shelf in our mean Látrabjarg hydrographic section (Fig. 3). However, the EG SHELF particle group also indicates that some of the dense water passing through the deepest part of Denmark Strait undergoes excursions onto the shelf downstream of the sill, and subsequently cascades back off the shelf at some later time into the Spill Jet. Most of the EG SHELF particles become less dense as they enter the Spill Jet (Fig. 8b), but

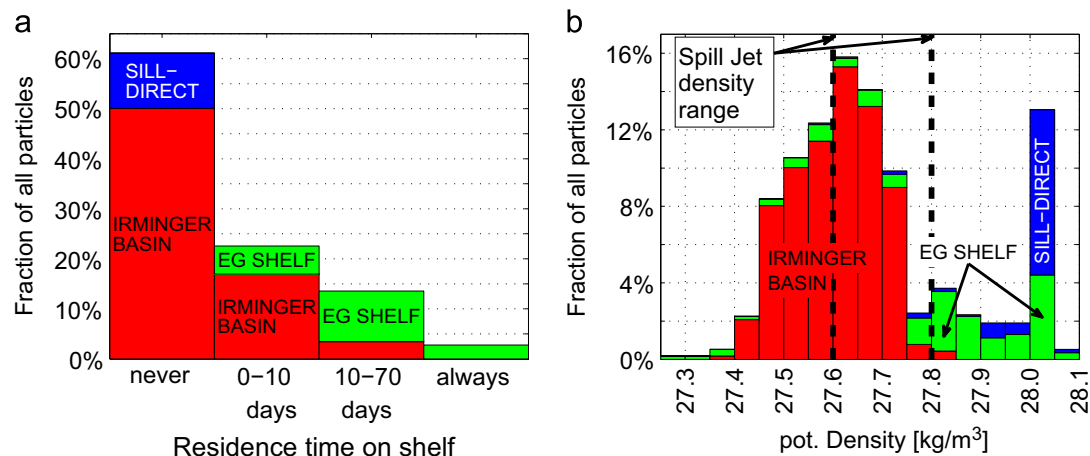


Fig. 8. Statistics of the numerical particles. (a) Fraction of all particles as a function of their residence time on the East Greenland shelf and their pathway group. (b) Fraction of all particles as a function of their potential density at the beginning of the simulation and their pathway group. The density range of the Spill Jet (27.6–27.8) is denoted by the dashed lines.

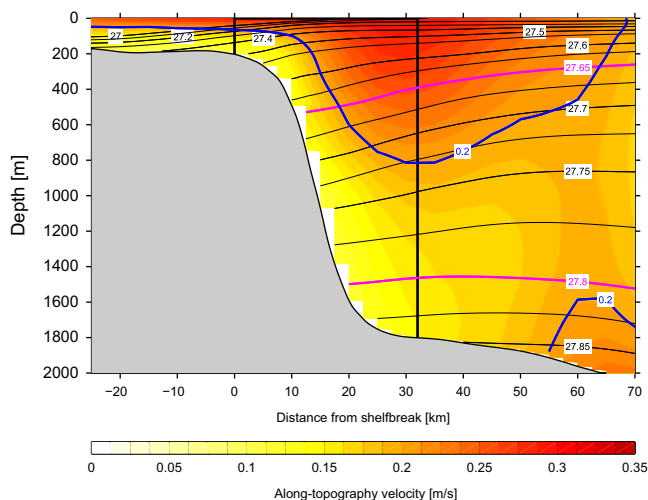


Fig. 9. Mean hydrography and velocity at the Cape Farewell section. The means are based on 36 CTD sections. The equatorward absolute geostrophic velocity is shown in color and the blue contour and is overlain by potential density (kg/m³) in black contours. The Spill Jet contribution is defined as the flow within 32 km of the shelfbreak (vertical black lines) in the density range 27.65–27.8 (magenta isopycnals). The absolute geostrophic velocity is referenced to shipboard ADCP data and AVISO absolute sea surface height. (For interpretation of the references to color in this figure caption, the reader is referred to the web version of this paper.)

a small portion becomes heavier, presumably by mixing with dense water from the direct slope pathway noted above.

Finally, the numerical model suggests that the majority of the water in the Spill Jet, about 70%, originates from the Irminger Basin (the IRMINGER BASIN group, Fig. 8a). This underscores the importance of entrainment in setting the transport and final water properties of the Spill Jet. However, while water from the Irminger Basin makes up the majority of the volume in the Spill Jet, the other two origin groups provide the excess density required for the dynamical processes leading to the formation of the Spill Jet. This is consistent with previous studies (e.g. Pickart et al., 2005; Falina et al., 2012) that emphasized the importance of the dense water sources without exploring the sources of the entrained water in detail. It is also consistent with observations indicating that the Spill Jet is characterized by low Richardson numbers indicative of strong mixing (Brearley et al., 2012). According to the model, the density of the IRMINGER BASIN particles increases on average by 0.1 kg/m^3 as they enter the Spill Jet (Fig. 8b). The

IRMINGER BASIN particles originate from the warm, salty Irminger Current along the northwest flank of the Reykjanes Ridge in water depths less than 2200 m (Fig. 6) at a depth horizon of approximately 750 m (not shown). The stratification and the temperature–salinity properties in this region are distinct from the interior Irminger Sea (Pickart et al., 2003, 2005), which is partly filled with weakly stratified Labrador Sea Water (LSW) formed by open ocean convection (Pickart et al., 2003; Yashayaev et al., 2007). Consequently, we conclude that appreciable amounts of LSW are not entrained into the Spill Jet.

5. Fate of the Spill Jet and its role in the large-scale circulation

The observations and modeling presented here of a ubiquitous Spill Jet on the upper continental slope south of Denmark Strait have quantified a new component of the boundary current system of the northern Irminger Sea. An obvious next question is the following: What is the fate of the $> 3 \text{ Sv}$ of intermediate density water transported southward by the Spill Jet and hence how does the Spill Jet fit into the regional circulation of the Irminger Sea? To address this, we make use of the previously constructed mean hydrographic/velocity section of 36 shipboard crossings of the boundary current system near Cape Farewell, Greenland (Våge et al., 2011) (Fig. 1). We note that the DSOW cyclones do not reach this latitude (Våge et al., 2011; Danialt et al., 2011). The mean velocity at Cape Farewell shows no evidence of the bottom-intensified Spill Jet observed upstream (Fig. 9). Instead, one sees the well-known surface-intensified EGC/IC seaward of the shelfbreak, and the top portion of the traditional DSOW in the DWBC (which extends deeper and farther offshore, and is only partly visible in Fig. 9). It has been argued previously that the mixing between the cold, fresh water spilling off the shelf south of Denmark Strait and the warm, salty water in the Irminger Basin leads to double diffusive salt fingering (Brearley et al., 2012). This erodes the cross-slope temperature gradient of the Spill Jet more effectively than the salinity gradient. As a consequence, the isopycnal slope of the Spill Jet should reverse as the current progresses southward, resulting in weaker flow with depth as seen in Fig. 9.

We expect that the boundary current system does not reduce its volume transport progressing downstream. However, distinguishing the Spill Jet from the other flow components becomes more difficult. With this in mind, we compute the volume transport at the Cape Farewell section within the density range 27.65–27.8. As before, the lower isopycnal is the top of the DSOW.

The upper isopycnal is chosen to exclude the warm and salty shallow core of the EGC/IC. There is, however, no obvious way to choose the offshore limit of the Spill Jet. Instead, we ask what is the lateral bound if the Spill Jet transport of 3.3 Sv remains the same south of 65°N (based on synoptic sections, Pickart et al. (2005) concluded that further entrainment is minimal south of the Spill Jet section). In this case, the offshore boundary is located at 32 km (Fig. 9). This is essentially what we would expect, that is, the Spill Jet occupies the inshore side of the deep equatorward-flowing jet at Cape Farewell.

The signature of the surface-intensified EGC/IC near the southern tip of Greenland (and into the Labrador Sea) has been recognized for decades (Buch, 1984). Historically, the deep portion of this current has been considered to be part of the lateral circulation of the North Atlantic sub-polar gyre. Our results indicate, however, that the flow in fact includes a significant fraction of the mid-depth component of the AMOC. There are numerous ramifications associated with this discovery. For example, the density range under consideration is the same as for Labrador Sea Water (LSW) formed in the Labrador Basin, which is traditionally considered to be the major contributor to the mid-depth AMOC (Talley et al., 2003). Since the total AMOC transport is well constrained (Schmitz and McCartney, 1993), our study questions this notion by identifying another large source of this water outside of the Labrador Sea. Estimates of the LSW formation rate vary widely, and based on 33 different published estimates in the literature, the mean value is 4.8 ± 2.6 Sv (Haine et al., 2008). However, calculating the local sinking rate in the Labrador Sea is difficult, and the sole direct estimate using velocity data is just 1 Sv (Pickart and Spall, 2007). The Spill Jet volume transport of 3.3 ± 0.7 Sv reported here thus accounts for a large fraction of the water in the LSW density range of the AMOC. Another important point is that the ventilation process for the Spill Jet takes place in the Nordic Seas and the entrainment into the jet occurs in the northern Irminger Basin. This is a very different set of mechanisms than that associated with the formation of LSW in the Labrador Sea. The Spill Jet therefore likely exhibits different sensitivity to climate change than traditional LSW, and climate scientists will need to re-assess the response of the mid-depth component of the AMOC to trends in atmospheric forcing (e.g. warmer air temperatures) and surface freshwater fluxes (e.g. enhanced ice-melt and runoff). Finally, our study implies that there is a tighter link between the deep and mid-depth components of the AMOC, since dense water passing through the deepest part of Denmark Strait can feed either the Spill Jet or the Deep Western Boundary Current. Further research is required to sort out this link and understand the consequences in the light of global warming.

Acknowledgements

We thank many individuals who helped collect and process the hydrographic data from the Denmark Strait, including Detlef Quadfasel, Torsten Kanzow, Bert Rudels, Rolf Käse, and Tom Sanford. Kjetil Våge shared the mean Cape Farewell sections for the analysis. Support for this study was provided by the U.S. National Science Foundation (OCE-0726640, OCI-1088849, OCI-0904338), the German Federal Ministry of Education and Research (OF0651 D), and the Italian Ministry of University and Research through the RITMARE Flagship Project.

Appendix A. Supplementary material

Supplementary Movie 1 associated with this paper can be found in the online version at <http://dx.doi.org/10.1016/j.dsr.2014.06.002>.

References

- Adcroft, A., Campin, J.-M., 2004. Rescaled height coordinates for accurate representation of free-surface flows in ocean circulation models. *Ocean Model.* 7 (3), 269–284.
- Brearely, J., Pickart, R., Valdimarsson, H., Jónsson, S., Schmitt, R., Haine, T.W.N., 2012. The East Greenland boundary current system south of Denmark Strait. *Deep Sea Res.* 1 63 (1), 1–19.
- Buch, E., 1984. Variations in temperature and salinity of West Greenland waters, 1970–82. *NAFO Sci. Council Stud.* 7, 39–44.
- Chassignet, E.P., Hurlburt, H.E., Metzger, E.J., Smedstad, O.M., Cummings, J.A., Halliwell, G.R., Bleck, R., Baraille, R., Wallcraft, A.J., Lozano, C., et al., 2009. US GODAE: global ocean prediction with the HYbrid Coordinate Ocean Model (HYCOM). *Oceanography* 22 (2), 64–76.
- Daniault, N., Lherminier, P., Mercier, H., 2011. Circulation and transport at the southeast tip of Greenland. *J. Phys. Oceanogr.* 41, 437–457.
- Dickson, R., Brown, J., 1994. The production of North Atlantic deep water: sources, rates, and pathways. *J. Geophys. Res.* 99 (C6), 12319–12341.
- Falina, A., Sarafanov, A., Mercier, H., Lherminier, P., Sokov, A., Daniault, N., 2012. On the cascading of dense shelf waters in the Irminger Sea. *J. Phys. Oceanogr.* 42 (12), 2254–2267.
- Haine, T.W.N., 2010. High-frequency fluctuations in Denmark Strait transport. *Geophys. Res. Lett.* 37 (14), L14601.
- Haine, T.W.N., Böning, C., Brandt, P., Fischer, J., Funk, A., Kieke, D., Kvaleberg, E., Rhein, M., Visbeck, M., 2008. North Atlantic deep water formation in the Labrador Sea, recirculation through the subpolar gyre, and discharge to the subtropics. In: *Arctic-Subarctic Ocean Fluxes: Defining the Role of the Northern Seas in Climate*. Springer, Dordrecht, The Netherlands, pp. 653–701 (Chapter 27).
- Harden, B., Pickart, R., Renfrew, I.A., 2014. Offshore transport of dense water from the East Greenland shelf. *J. Phys. Oceanogr.* 44 (1), 229–245.
- Holliday, N., Bacon, S., Allen, J., McDonagh, E., 2009. Circulation and transport in the western boundary currents at Cape Farewell, Greenland. *J. Phys. Oceanogr.* 39 (8), 1854–1870.
- Jochumsen, K., Quadfasel, D., Valdimarsson, H., Jónsson, S., 2012. Variability of the Denmark Strait overflow: Moored time series from 1996–2011. *J. Geophys. Res.* 117 (C12).
- Kalnay, E., Kanamitsu, M., Kistler, R., Collins, W., Deaven, D., Gandin, L., Iredell, M., Saha, S., White, G., Woollen, J., et al., 1996. The NCEP/NCAR 40-year reanalysis project. *Bull. Am. Meteorol. Soc.* 77 (3), 437–471.
- Käse, R., Girtton, J., Sanford, T., 2003. Structure and variability of the Denmark Strait overflow: model and observations. *J. Geophys. Res.* 108 (C6), 3181.
- Koszalka, I., Haine, T.W.N., Magaldi, M., 2013. Fates and travel times of Denmark Strait overflow water in the Irminger Basin. *J. Phys. Oceanogr.* 43 (12), 2611–2628.
- Large, W.G., McWilliams, J.C., Doney, S.C., 1994. Oceanic vertical mixing: a review and a model with a nonlocal boundary layer parameterization. *Rev. Geophys.* 32 (4), 363–403.
- Lherminier, P., Mercier, H., Huck, T., Gourcuff, C., Perez, F.F., Morin, P., Sarafanov, A., Falina, A., 2010. The Atlantic meridional overturning circulation and the subpolar gyre observed at the A25-OVIDE section in June 2002 and 2004. *Deep Sea Res.* 1 57 (11), 1374–1391.
- Macrander, A., Send, U., Valdimarsson, H., Jónsson, S., Käse, R., 2005. Interannual changes in the overflow from the Nordic Seas into the Atlantic Ocean through Denmark Strait. *Geophys. Res. Lett.* 32 (6), L06606.
- Magaldi, M., Haine, T.W.N., Pickart, R., 2011. On the nature and variability of the East Greenland spill jet: a case study in summer 2003. *J. Phys. Oceanogr.* 41 (12), 2307–2327.
- Nikolopoulos, A., Pickart, R., Fratantoni, P., Shimada, K., Torres, D., Jones, E., 2009. The western Arctic boundary current at 152°W: structure, variability, and transport. *Deep Sea Res.* 1 56 (17), 1164–1181.
- Pickart, R., Smethie, W., 1998. Temporal evolution of the deep western boundary current where it enters the sub-tropical domain. *Deep-Sea Res.* 1 45 (7), 1053–1083.
- Pickart, R., Spall, M., 2007. Impact of Labrador Sea convection on the north Atlantic meridional overturning circulation. *J. Phys. Oceanogr.* 37 (9), 2207–2227.
- Pickart, R., Straneo, F., Moore, G., 2003. Is Labrador Sea water formed in the Irminger Basin? *Deep-Sea Res.* 1 50 (1), 23–52.
- Pickart, R., Torres, D., Fratantoni, P., 2005. The East Greenland spill jet. *J. Phys. Oceanogr.* 35 (6), 1037–1053.
- Price, J., O’Neil Baringer, M., 1994. Outflows and deep water production by Marginal Seas. *Prog. Oceanogr.* 33 (3), 161–200.
- Rudels, B., Eriksson, P., Grönvall, H., Hietala, R., Launiainen, J., 1999. Hydrographic observations in Denmark Strait in Fall 1997, and their implications for the entrainment into the overflow plume. *Geophys. Res. Lett.* 26 (9), 1325–1328.
- Sarafanov, A., Falina, A., Mercier, H., Sokov, A., Lherminier, P., Gourcuff, C., Gladyshev, S., Gaillard, F., Daniault, N., 2012. Mean full-depth summer circulation and transports at the northern periphery of the Atlantic Ocean in the 2000s. *J. Geophys. Res.* 117 (C1).
- Schmitz, W.J., McCartney, M.S., 1993. On the north Atlantic circulation. *Rev. Geophys.* 31 (1), 29–49.
- Smith, P., 1975. A streamtube model for bottom boundary currents in the ocean. *Deep Sea Res.* 1 22 (12), 853–873.
- Spall, M., Price, J., 1998. Mesoscale variability in Denmark Strait: the PV outflow hypothesis. *J. Phys. Oceanogr.* 28 (8), 1598–1623.

- Talley, L.D., Reid, J.L., Robbins, P.E., 2003. Data-based meridional overturning streamfunctions for the global ocean. *J. Clim.* 16 (19), 3213–3226.
- Våge, K., Pickart, R.S., Sarafanov, A., Knutsen, Ø., Mercier, H., Lherminier, P., VanAken, H.M., Meincke, J., Quadfasel, D., Bacon, S., 2011. The Irminger gyre: circulation, convection, and interannual variability. *Deep Sea Res. I* 58 (5), 590–614.
- von Appen, W.J., 2012. Moored Observations of Shelfbreak Processes at the Inflow to and Outflow from the Arctic Ocean (Ph.D. thesis). Massachusetts Institute of Technology and Woods Hole Oceanographic Institution, Cambridge/Woods Hole, MA.
- von Appen, W.J., Pickart, R., Brink, K., Haine, T.W.N., 2014. Water column structure and statistics of Denmark Strait overflow water cyclones. *Deep Sea Res. I* 84, 110–126.
- Yashayaev, I., Bersch, M., van Aken, H.M., 2007. Spreading of the Labrador Sea Water to the Irminger and Iceland basins. *Geophys. Res. Lett.* 34 (10).